JMEPEG (2009) 18:1226–1229
DOI: 10.1007/s11665-009-9377-y

1059-9495/$19.00

Microstructure and Properties of Homogeneous and Gradient Ti(C, N) Coatings

Dai-hong Xiao

(Submitted June 6, 2008; in revised form January 24, 2009)

The microstructure and properties of homogeneous and gradient Ti(C, N) coatings synthesized using magnetron sputtering technique were investigated using x-ray diffraction (XRD), scanning electron microscopy (SEM), secondary ion mass spectroanalyzer (SIMS), nanoindentation, and cutting tests. The results have shown that the coatings between homogenous and gradient Ti(C, N) are face centered cubic structure and show the columnar crystallites. The homogeneous Ti(C, N) exhibits higher nanohardness compared to the gradient Ti(C, N) coating. Moreover, the homogeneous Ti(C, N) coated inserts behave better wear resistance in continuous turning but worse properties in interrupted cutting.

Keywords microstructure, properties, Ti(C, N) coating

1. Introduction

Important criteria for the use of materials in tribological applications are sufficient adhesion, high hardness and toughness, resistance against oxidation, and a low friction coefficient (Ref 1). TiN coating has successfully been employed as wear-resistant coatings in many fields for their high hardness, low wear coefficient, and other good properties (Ref 2, 3).

To improve the coatings hardness and other properties further, Al, C, Cr, and Si are added to form (Ti, Al)N, Ti(C, N), TiAlCrN, and Ti-Si-N composite coatings (Ref 4-9). The multiphase Ti(C, N) thin coating, combining the advantages of the high hardness of TiC and the high ductility and adhesion strength of TiN, possesses better comprehensive mechanical properties than single-phase TiC or TiN (Ref 10-12). However, due to the difference in the microstructure and properties of the thin hard coating and those of the underlying soft substrates, it is very likely that the stress will concentrate in the boundary between substrate and coatings during deformation, which ultimately leads to crack formation and delamination of the coating from substrate. The sharp interface between the coating and substrate may be eliminated by introducing the concept of functionally gradient material (FGM) in the design of the coating (Ref 13-16). The compositions, microstructures, and properties of FGM change continuously from one side to the other side. It is helpful in increasing the adhesion strength between coating and substrate as well. This may be explained based on the distribution of stress and strain at the interface and within the coating with a gradient in elastic modulus (Ref 17, 18).

D. Xiao, State Key Laboratory of Powder Metallurgy, Central South University, Changsha 410083, China. Contact e-mail: xdh0615@163.com.

In this paper, we present results from a study on the homogeneous and gradient coatings deposited by physical vapor deposition. The aim of the experiments is to investigate the coating composition and structure.

2. Experimental

The substrate materials in this experiments were WC-6 wt.% Co sintered cemented carbides. After milling and drying, the mixtures of WC and Co powders were pressed to TNMG120408 inserts and sintered in vacuum. Homogeneous and gradient Ti(C, N) coatings with a nominal thickness of about 3 μm were deposited onto the mirror-polished substrates at 350 °C by means of magnetron sputtering technique. The sputter target was pure titanium (99.5%). High purity argon (99.99%) was the sputtering gas, while nitrogen and ethyne (purity of 99.99%) were used as reactive gas. The base pressure in the chamber was <0.5 mPa, and the working pressure consisting of Ar, N_2, and C_2H_2 was set at 580 MPa during the deposition process. Before deposition, the target was cleaned by Ar glow discharge and a thin pure Ti layer was first deposited in order to improve the coating adhesion to the substrate. In the process of the homogeneous Ti(C, N) coating deposition, the reactive gas is a mixture gas of N_2 and C_2H_2 with a gas-flow rate of 200 sccm for N_2 and 20 sccm for C_2H_2. During the gradient Ti(C, N) coating deposition process, the N_2 flux decreases from 250 to 80 sccm while the C_2H_2 flux increases from 0 to 30 sccm. C_2H_2, the reactive gas, was also admitted discontinuously into the vacuum chamber with reactive gas N_2.

The phase identification for the coatings was performed using XRD (Bruker D8). The diffraction experiments were performed on a 2 Θ/Ω diffractometer at a small angle of incidence of the primary beam ($\gamma = 30$) and with a nearly parallel diffraction beam. The microstructure of the as-deposited coatings was observed by means of SEM (JSM-6360LV) instruments with operating volts of 20 kV. The elemental distribution of gradient Ti(C, N) coating was analyzed by typical secondary ion mass spectroanalyzer (SIMS).

A two-step penetration method with nanoindentation was used to measure the nanohardness of the coatings with a computer-controlled nanoindentation tester (Fischerscope H100VP) using a Vickers indenter and continuously applied load. A maximum load with holding time of 10 s was selected to measure the nanohardnesses of the films. A smaller penetration load of 5 mN was chosen to measure the mechanical properties of the coatings because such a low load could ensure that the deformation under the indentation tip is controlled within the films and the substrate effect can be avoided. The Vickers hardness HV is computed from the load/unload displacement curves by adopting Oliver and Pharr formula. In this step, as many as 20 indentations were performed on each specimen.

One method for evaluating the properties of coatings inserts is the measurement of flank wear. In the present test, the resistance to abrasion was compared by continuous turning of stainless steel (1Cr18Ni9Ti) with TNMG120408 style insert, the cutting conditions were a cutting speed (vc) of 160 m/s, a depth of cut (ap) of 2×10^{-4} m and a feed rate (f) of 2×10^{-4} m/r. Flank wear lands were measured using a microscope in interval 2 min and the inserts were deemed as failure when the wear lands exceeded 3×10^{-4} m.

The impact resistance of coated inserts was investigated using the interrupted cutting of carbon steel containing 0.45% C. Coated inserts were tested under cutting conditions with interrupted material removal, using a four-gutters machining center and cylindrical workpieces. The nose of insert is impacted four times at a cutting circuit. Calculating the nose impact times expressed the impact resistance. The cutting conditions were a rotation speed of 2.1×10^4 r/h, a depth of cut (ap) of 2×10^{-4} m, and a feed rate (f) of 2×10^{-4} m/r. Nose wear lands were measured using a microscope every 2 min. An end-of-life criterion for the inserts was the nose wear exceed 0.5 mm.

3. Results

Figure 1 showed XRD patterns of the homogeneous and gradient Ti(C, N) coatings. Both coatings possess polycrystalline diffraction peaks related to the face centered cubic structure. Compared with homogeneous Ti(C, N) coating, the peak positions of gradient Ti(C, N) coating are shifted to higher angle. It is notable that there is obvious orientational difference between the two coatings. Table 1 shows texture coefficient of two coatings. The texture coefficients of the different coatings are calculated from their respective XRD peaks using the following formula:

$$\text{Texture coefficient} = I(hkl)/[I(111) + I(200)]$$

where *hkl* represents the (111), (200), or (220) orientations.

The texture coefficients of the (200) and (111) orientation in the homogeneous Ti(C, N) coating are lower than that of the gradient Ti(C, N) coating. However, the (220) preferred orientation for the gradient Ti(C, N) coating is weaker compared to that of the homogeneous Ti(C, N) coating.

Figure 2 shows the SEM images of fractured cross sections of homogeneous and gradient Ti(C, N) coatings. Both coatings have dense columnar structures with most of grains extending from the interface to the surface. Secondary ion mass spectroanalyzer analysis show the relative content of C increases but

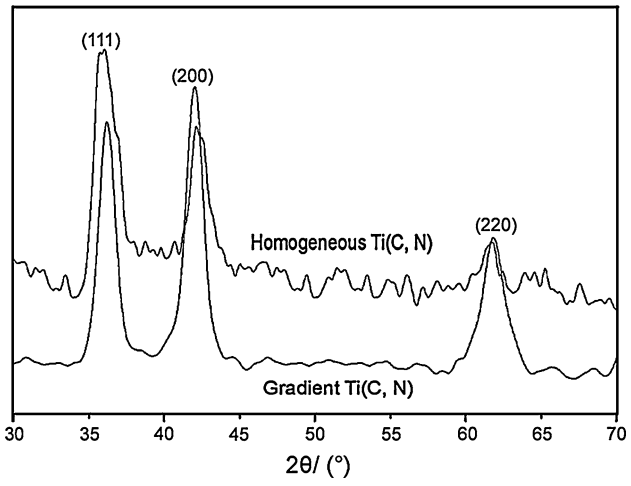

Fig. 1 XRD patterns of homogeneous and gradient Ti(C, N) coatings

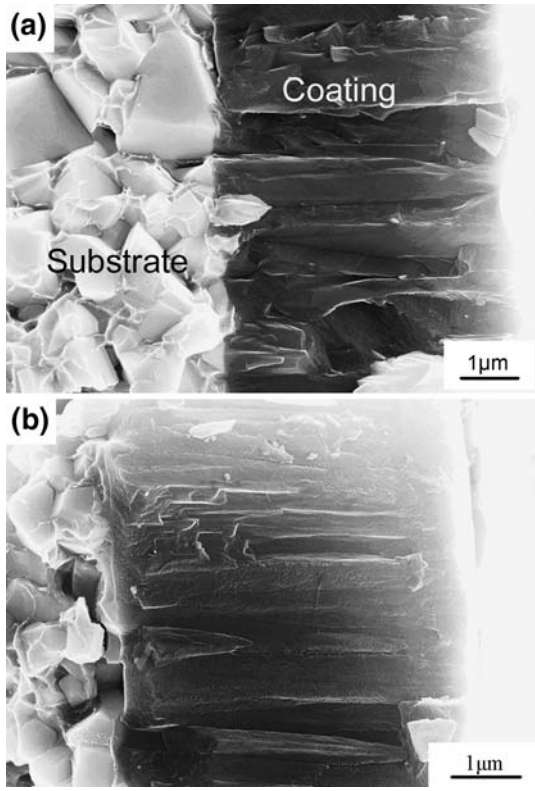

Fig. 2 SEM images of fractured cross sections of coatings. (a) Homogeneous Ti(C, N) coating and (b) gradient Ti(C, N) coating

Table 1 Texture coefficient of homogeneous and gradient Ti(C, N) coatings

	Texture coefficient *T**		
Coating technology	**(111)**	**(200)**	**(220)**
Homogeneous Ti(C, N)	0.8059	0.2700	1.9450
Gradient Ti(C, N)	1.28516	0.66343	1.06974

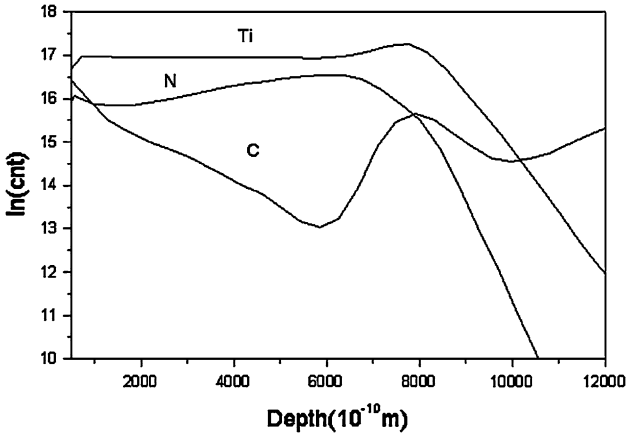

Fig. 3 SIMS graphs of gradient Ti(C, N) coating

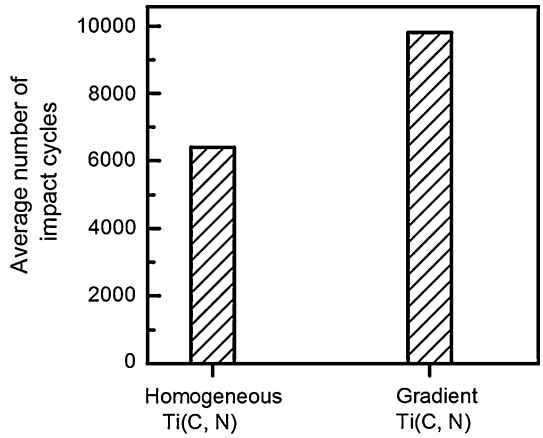

Fig. 5 Tools life of coated inserts in interrupted machining of carbon steel containing 0.45% C

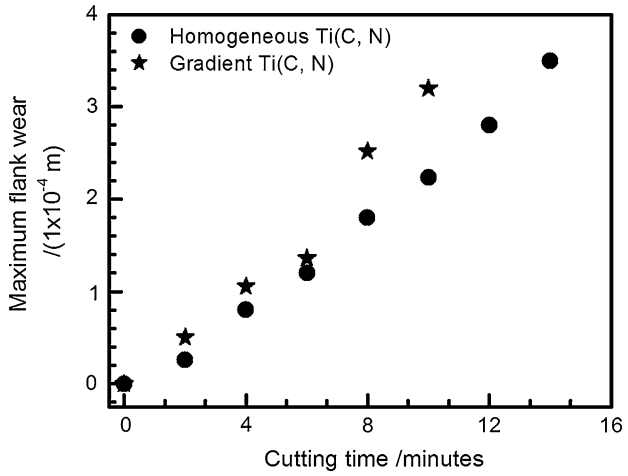

Fig. 4 The progress of flank wears of coated inserts in continuous turning stainless steel

N decreases in increasing coating thickness for gradient Ti(C, N) coating (Fig. 3). The C content near the substrate sharply rises from the C content in the cemented carbide substrate. A Ti-rich transition layer formed during Ti ions pretreatment on the substrate is also observed in the interface between the coating and the substrate.

The measured nanohardness values for the homogeneous Ti(C, N) and gradient Ti(C, N) coatings are 34.6 and 28.7 GPa respectively. Compared to the homogeneous Ti(C, N) coating, the nanohardness value for the gradient Ti(C, N) coating is lower.

The metal cutting properties of coated tools are a function of substrate, coating, and geometry of the cutting edge. For the given metal cutting test, we kept the substrate and the geometry constant. Therefore, the tool life differences observed in the test should be only to the differences in the properties of the coated materials and their adhesion to the substrate. Maximum flank wear as a function of time at a cutting speed of 160 m/s in turning stainless steel (1Cr18Ni9Ti) is shown in Fig. 4. The properties of the homogeneous Ti(C, N) coated inserts were superior to the gradient Ti(C, N) coated inserts.

Figure 5 demonstrates the tools lifetimes of the different coated inserts in interrupted cutting of carbon steel containing 0.45% C at a speed of 350 r/min, which were determined by the average impact times of inserts. The failure criterion for the inserts was a critical size of wear land as mentioned in Section 2. The average impact times of the inserts with the homogeneous Ti(C, N) and gradient Ti(C, N) coats were 9800 and 6400 times, respectively. Compared to the homogeneous Ti(C, N) coated inserts under the same working conditions, the gradient Ti(C, N) coated inserts achieve around 53% improvement.

4. Discussion

As shown in Fig. 1, the XRD spectra revealed a strong (111) preferred orientation in the homogeneous and gradient Ti(C, N) coatings (Fig. 1). In general, magnetron sputtering deposition is a high energy process and evaporated titanium ions are believed to have energies between 50 and 100 eV (Ref 19). In addition to this intrinsic energy of titanium ions, the substrates were negatively biased to −100 V during all depositions with the effect of increasing ion energies even further. It is well known (Ref 20) that TiN/TiC film formation under high ion energy bombardment favors the growth of densely packed atomic planes.

The texture coefficients of the (200) and (111) orientation in the gradient Ti(C, N) coating are higher than those of the homogeneous Ti(C, N) coating (Table 1). Moreover, the peak position of the gradient Ti(C, N) coasting is shifted to higher angle with respect to the homogeneous Ti(C, N) coating. The shift in peak position of the gradient Ti(C, N) coating may be due to lattice constant decreases arise from the partial replacement of the titanium atoms in the TiN lattice by the carbon.

It is also shown that the nanohardness value of the homogeneous Ti(C, N) coating is higher than that of the gradient Ti(C, N). The hardness enhancement in the homogeneous Ti(C, N) coating is due to the low carbon content. In addition, the solution hardening in the homogeneous Ti(C, N) coating may be contributing to the hardness enhancement.

The metal cutting test (Fig. 4) showed that the properties of the homogeneous Ti(C, N) coated insert was superior to the gradient Ti(C, N) coated inserts. The reason for this is the higher hardness of the homogeneous Ti(C, N) coating. However, the average impact time of the insert with the

gradient Ti(C, N) coating is superior to the homogeneous Ti(C, N) coating. This is due to the better adhesion with substrate of the gradient Ti(C, N) coating suppresses microcracks initiation in a certain extent compared with the homogeneous Ti(C, N) during interrupted cutting. In addition, the gradient zone can absorb the energy of cracks propagation and prevent the cracks from propagating, which definitely improve cutting edge toughness and impact resistance of the coated inserts. Thus, it is possible that the homogeneous Ti(C, N) coated inserts are fit for turning and the gradient Ti(C, N) coated inserts are fit for milling in machining.

5. Conclusions

Both sputtered homogeneous and gradient Ti(C, N) coatings have the face centered cubic structure and dense columnar structures with most of grains extending from the interface to the surface. The homogeneous Ti(C, N) coating exhibits higher nanohardness than that of the gradient Ti(C, N). Moreover, the homogeneous Ti(C, N) coated inserts have better wear resistance than gradient Ti(C, N) coated inserts in continuous turning. But the gradient Ti(C, N) coated inserts showed the better properties in interrupted cutting. So we can choose the coating technology in accordance with different machining state.

Acknowledgments

This work was supported by the Foundation for the Innovative Research Groups of the National Natural Science Foundation of China (No. 50721003) and the Special Foundation of Postdoctoral Research Foundation of China (No. 200801348). Useful comments by an anonymous reviewer are also acknowledged.

References

1. S. Veprek and S. Reiprich, Concept for the Design of Novel Superhard Coatings, *Thin Solid Films*, 1995, **268**, p 64–71
2. E. Bergman, H. Kaufmann, R. Schmid, R. Schmid, and J. Vogel, Ion-plated Titanium Carbonitride Films, *Surf. Coat. Technol.*, 1990, **42**, p 237–251
3. H. Holleck, Material Selection for Hard Coatings, *J. Vac. Sci. Technol.*, 1986, **A4**, p 2661–2664
4. I.W. Park and K.H. Kim, Coating Materials of TiN, Ti-Al-N, and Ti-Si-N by Plasma-enhanced Chemical Vapor Deposition for Mechanical Applications, *J. Mater. Process. Technol.*, 2002, **130–131**, p 254–259
5. Ch. Taschner, B. Ljunqberq, V. Hoffman, C. Vogt, and A. Leonhardt, Deposition of TiN, TiC and $Ti_{1-x}Al_xN$ Coatings by Pulsed d.c. Plasma Enhanced Chemical Vapour Deposition Methods, *Surf. Coat. Technol.*, 2001, **142–144**, p 823–828
6. M. Zlatanovic, I. Popovic, and S. Zlatanovic, Structural, Mechanical and Optical Properties of TiN and (Ti, Al)N Coatings, *Mater. Sci. Forum.*, 2000, **352**, p 35–42
7. S. PalDey and S.C. Deevi, Single Layer and Multilayer Wear Resistant Coatings of (Ti, Al)N: A Review, *Mater. Sci. Eng.*, 2003, **A342**, p 58–79
8. A. Kovalev, D.L. Wainstein, K. Yamamoto, G. Fox-Rabinovich, K. Yamamoto, and S. Veldhius, Impact of Al and Cr Alloying of TiN-based PVD Coatings on its Cutting Performance, *Surf. Interface Anal.*, 2006, **39**, p 879–882
9. P.H. Mayrhofer, C. Mitterer, L. Hultman, and H. Clemens, Micro-structural Design of Hard Coatings, *Prog. Mater. Sci.*, 2006, **51**, p 1032–1114
10. H. Randhawa, Cathodic Arc Plasma Deposition of TiC and TiC_xN_{1-x} Films, *Thin Solid Films*, 1987, **153**, p 209–218
11. E. Damond, P. Jacquot, and J. Pagny, TiC_xN_{1-x} Coatings by Using the Arc Evaporation Technique, *Mater. Sci. Eng.*, 1991, **A140**, p 838–841
12. P. Huber, D. Manova, S. Mandl, and B. Rauschenbach, Formation of TiN, TiC and TiCN by Metal Plasma Immersion Ion Implantation and Deposition, *Surf. Coat. Technol.*, 2003, **174–175**, p 1243–1247
13. K. Narasimhan, S.P. Boppana, and D.G. Bhat, Development of a Graded TiCN Coating for Cemented Carbide Cutting Tools—A Design Approach, *Wear*, 1995, **188**, p 123–129
14. H.K. Tönshoff and H. Seegers, Influence of Residual Stress Gradients on the Adhesion Strength of Sputtered Hard Coatings, *Thin Solid Films*, 2000, **377–378**, p 340–345
15. I. Dahan, U. Admon, N. Frage, J. Sariel, M.P. Dariel, and J.J. Moore, The Development of a Functionally Graded TiC-Ti Multilayer Hard Coating, *Surf. Coat. Technol.*, 2001, **137**, p 111–115
16. U. Schulz, M. Peters, F.W. Bach, and G. Tegeder, Graded Coatings for Thermal, Wear and Corrosion Barriers, *Mater. Sci. Eng.*, 2003, **A362**, p 61–80
17. I. Shiota, Fundamental Research on Functionally Gradient Materials (FGM) for Relaxation of Thermal Stress by TMS, *Proceedings from the Conference on Critical Issues in the Development of High Temperature Structural Materials* (Kona, USA), 1993, p 303–318
18. X.C. Zhang, B.S. Xu, H.D. Wang, Y. Jiang, and Y.X. Wu, Modeling of Thermal Residual Stresses in Multilayer Coatings with Graded Properties and Compositions, *Thin Solid Films*, 2006, **497**, p 223–231
19. A. Bendavid, P.J. Martin, G.B. Smith, L. Wielunski, and T.J. Kinder, Mechanical and Structural Properties of Ti films Prepared by Filtered Arc Deposition, *Vacuum*, 1996, **47**, p 1179–1188
20. G. Knuyt, C. Quaeyhaegens, J. D'Haen, and L.M. Stals, Model for Texture Evolution in a Growing Film, *Surf. Coat. Technol.*, 1995, **76–77**, p 311–315